CHAPTER 74

FIELD MEASUREMENTS OF SAND MOTION IN THE SURF ZONE

by

Douglas L. Inman; James A. Zampol; Thomas E. White
Daniel M. Hanes; B. Walton Waldorf; and Kim A. Kastens

Shore Processes Laboratory A-009
Scripps Institution of Oceanography
La Jolla, California 92093

ABSTRACT

Forcing functions and sediment response were measured during two comprehensive surf zone experiments. The experiments included simultaneous measurements of waves and currents, and the movement of sediment as bed and suspended load. The longshore transport of suspended load was found to be about 10 to 20% of the tracer-measured load. Results from tracer measurements of the longshore transport of bed load indicate that previous measurements may have misestimated the effective "tracer layer thickness," and a more rigorous method is proposed.

1. INTRODUCTION

There is extensive competition for the use of nearshore areas for harbors, recreational beaches and swimming, as recipients of thermal and waste discharges, and for coastal construction. Therefore, understanding of sediment transport processes has become essential to coastal technology.

As a consequence, the Nearshore Sediment Transport Study sponsored by the U.S. Office of Sea Grant, NOAA, and funded in part by the Office of Naval Research, has been engaged in extensive field experiments since 1977. The overall objective of the study is the development of improved engineering prediction techniques for sediment transport by waves and currents in the nearshore region. The studies have been conducted jointly by research teams from five universities. The first field experiments were carried out at Torrey Pines Beach near San Diego, California, in March 1977 and November-December 1978 (Gable (ed), 1979; Seymour and Gable, 1980). Additional experiments have recently been conducted near Santa Barbara, California, in February 1980.

The purpose of this paper is to present the results from the two most comprehensive, high energy experiments conducted on 11 March 1977 and 6 December 1978. These experiments included simultaneous measurement of forcing functions (i.e., waves, winds and currents) from sensor arrays in and outside the surf zone, as well as sediment response in terms of bed and suspended load movement.

2. TORREY PINES BEACH SITE

A portion of Torrey Pines Beach in San Diego County, California, was selected as a site for this study. The site is located 5.5 km north of Point La Jolla, and 4 km north of the ocean pier of the Scripps Institution of Oceanography. A 3.0 km segment of this beach that has gently sloping offshore bathymetry and is terminated shoreward by 100 meter high sea cliffs was used for the beach and nearshore measurements (Figure 2-1). This beach satisfied the basic requirements for a straight beach with uncomplicated offshore bathymetry that is exposed to waves from all offshore quadrants. Chamberlain (1960) and State of California (1969) have estimated the net littoral transport in the vicinity of Torrey Pines Beach at about 200,000 m^3 per year, to the south.

The study beach undergoes typical seasonal changes in configuration due to changes in wave climate. During summer wave conditions, the beach has a 30 to 60 meter wide backshore, a relatively steep upper foreshore, and a pronounced berm. Winter storm waves overtop the summer berm and erode the backshore, thus reducing the width of the exposed beach. Winter beach profile configuration is typified by a gently sloping beach foreshore that in places extends shoreward to the toe of the sea cliff. The beach profiles for the two experiments are shown in Figure 2-2. Generally the beach face slopes about 1:25, the surf zone 1:75, the section seaward to the 3 meter depth contour 1:35, while that portion from 3 to 10 meters depth slopes 1:50.

The sediments on the beach and shelf are predominantly fine quartz sand with minor amounts of feldspars and heavy minerals. Light minerals, that is those with a specific gravity of less than about 2.85, usually comprise 90% of the sample, while heavy minerals total about 10%. Of the light minerals approximately 88% is quartz, 10% feldspars and 2% shell fragments and miscellaneous material. Of the total heavy minerals hornblende is most plentiful, comprising about 60% (Inman, 1953). The size distributions for typical sediments obtained by grab samplers in the surf zone are listed in Table 2-1.

Table 2-1 Size distribution measures for sieved surf zone samples. Measures are from Inman (1952).

Date	11 March 1977			6 December 1978		
Measure	Md microns	σ_ϕ	α_ϕ	Md microns	σ_ϕ	α_ϕ
Inner	184	.37	0	152	.43	-.26
Middle	200	.39	+.18	157	.51	-.14
Outer	215	.47	+.17	152	.63	-.23

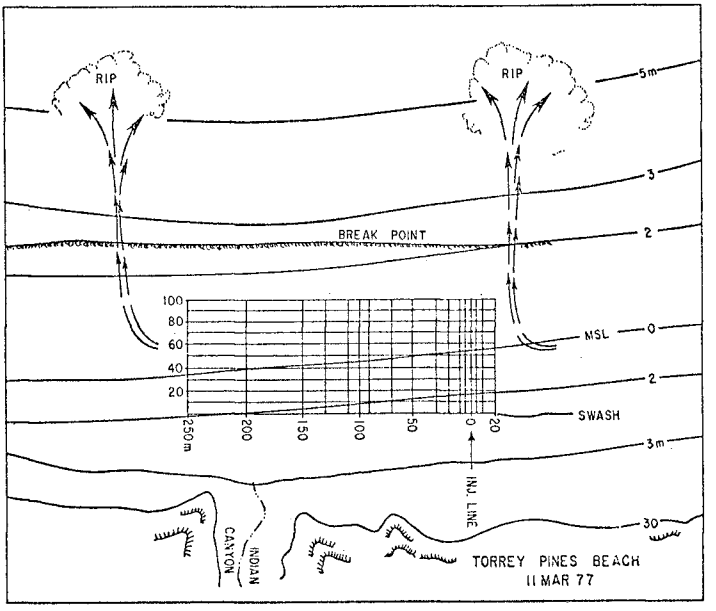

Fig. 2-1 Site and sampling grid for 11 March 77.

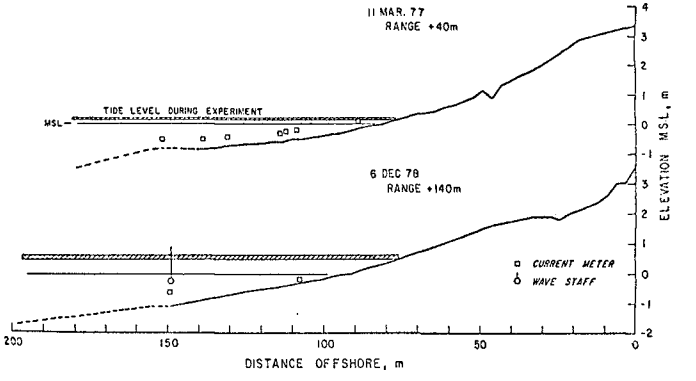

Fig. 2-2 Beach profiles and instrument locations for 11 March 77 and 6 December 78.

3. EXPERIMENT CONTROL

The dates and times of our tracer experiments were carefully selected to meet the following criteria: 1) fully operational status for the offshore wave array and other necessary sensors; 2) minimal change in tide elevation during a 3 hour period during daylight; 3) occurrence of dominant waves of sufficient height and breaker angle to generate a strong, unidirectional longshore current; and 4) absence of stationary rip currents across the sampling grid in the study area.

Figure 2-1 shows a stationary rip current pattern with separation between rip currents of 340 meters. In accordance with criterion 4, the injection line and sampling grid were placed within a 250 meter length of beach between rip currents. Reversal of longshore current during experiments resulted in the rejection of many of the experiments conducted on other days.

During the morning of the given day, Rhodamine-B dye was injected at several positions in the surf zone and observed from the cliff above the site. The dye dispersal patterns, such as that illustrated in Figure 4-4 indicated the approximate mean longshore current speed as well as the occurrence of complicating rip currents. If all conditions were satisfied, the injection location and sampling grid were determined appropriate to the current speed and direction, and flags marking the grid ranges were installed on the beach.

4. DRIVING FORCES

It is well known that the principal driving forces for longshore transport of sand in the nearshore waters are waves, currents, winds, and tides, in that order. Since strong winds did not occur during the two experiments described here, and because the experiments were scheduled to coincide with near still-stands in the tidal curve, neither wind nor tidal forces are considered to be important in these experiments. However, the stage of the tide may have some disequilibrium effect on the beach profile, as the water level during experiments was generally above mean sea level in order to cover the surf zone instruments. The tide in these waters is mixed, with a pronounced diurnal inequality. At the Scripps Institution of Oceanography pier the mean and spring tidal ranges are 3.6 and 5.2 feet (1.10 and 1.58 meters), and the mean tidal level is 2.7 feet (0.82 meters) above the datum of mean lower low water. During the experiments of 11 March 1977 and 6 December 1978 the water levels were about 20 cm and 60 cm respectively above mean tide level.

WAVES

The direction and flux of wave energy and momentum were measured from an array of wave pressure sensors placed parallel to shore in a water depth of 9.7 m below mean sea level, hereafter referred to as the 10 meter array. All data from it have been corrected to the actual depth of water at the times of the observations. Also, arrays of electromagnetic current meters, pressure sensors, and wave staffs were placed in and near the surf zone. Details of these near-surf arrays

are given in Guza and Thornton (1978, 1980) and Gable (ed 1979).

The spacings of the offshore line array were in a 1-2-4-5 and a 2-2-2-5 configuration with a unit lag of 33 meters and total array lengths of 396 and 363 meters respectively. The first was used on 11 March 1977 while the latter was used on 6 December 1978. The length of the array was designed for resolution of long period waves with directional peaks separated by 5^{o} to 10^{o} in ten meters of water. Data from the offshore array was telemetered back to the Shore Processes Laboratory of the Scripps Institution of Oceanography using the Shelf and Shore (SAS) system described by Lowe et al (1973).

The wave spectrum consists of the squares of the absolute values of the complex Fourier coefficients, which serve as estimates (having dimensions of length squared) of the energy density in each elemental frequency band. The sum of the energy densities under the spectral peak of the incident waves i.e., the variance, is the mean-square elevation $\langle \eta^2 \rangle$ of the water surface described by the time series. The mean wave energy per unit area of the water surface is given by the product of $\langle \eta^2 \rangle$ and the weight per unit volume ρg of the water,

$$E = \rho g \langle \eta^2 \rangle = \frac{1}{8} \rho g H^2_{rms} \qquad (4\text{-}1)$$

where H_{rms} is the root-mean-square wave height.

The energy spectrum was computed for time runs of about 17 minutes during which pressure was sampled two times per second (Δt = 0.5 sec), for a total number of data points n = 2048, which when transformed give 1024 elemental frequency bands. Energy and cross-spectra were computed from the summation of 8 (q = 8) elemental frequency bands, giving a total of 128 merged frequency bands and 16 degrees of freedom. The most important frequency bands were plotted, and examples are shown in Figures 4-1, 2.

Directional spectra were computed for every frequency band using the maximum likelihood estimator described by Capon (1969) and Davis and Regier (1977). Important frequency bands with high evergy peaks were graphed, and examples are shown in the lower part of Figures 4-1, 2.

There is in general a flux of energy in the direction of wave propagation, which in the absence of refraction and dissipation is a constant per unit width of wave crest

$$ECn = \left[ECn\right]_{\infty} = \text{const} \qquad (4\text{-}2)$$

where E is defined in relation (4-1), C is the wave phase velocity, and Cn is the wave group velocity.

Waves also transport momentum which is a tensor quantity consisting

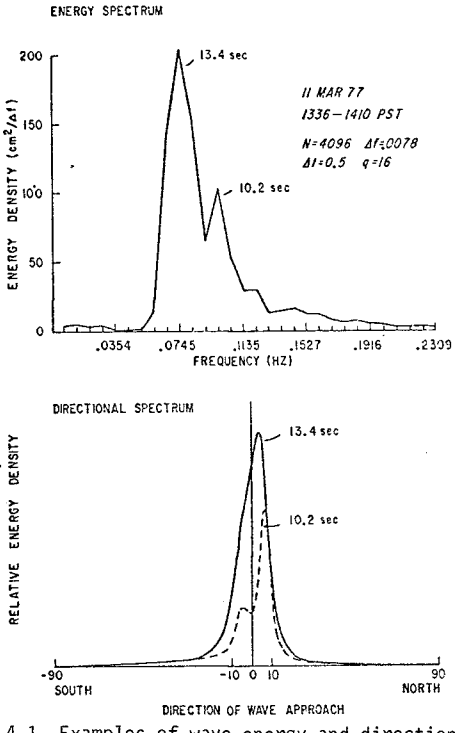

Fig. 4-1 Examples of wave energy and directional spectra for 11 March 1977.

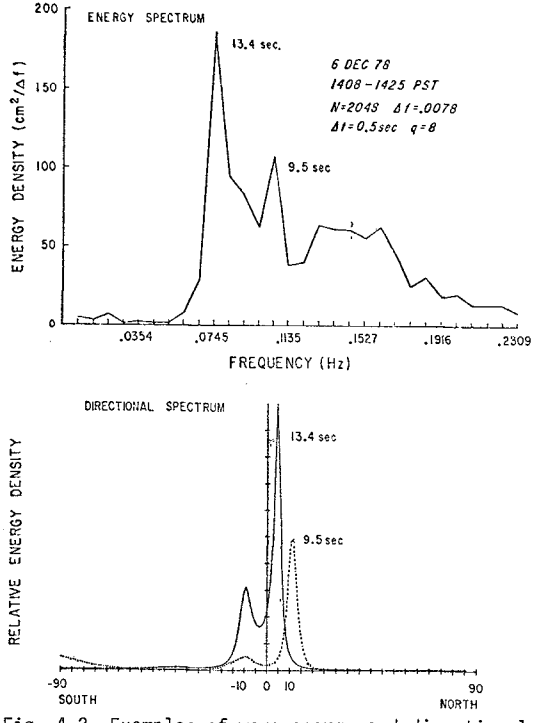

Fig. 4-2 Examples of wave energy and directional spectra for 6 December 1978.

of four components. The onshore flux of y-directed momentum S_{yx} has been shown to drive the longshore currents inside the surf zone (Bowen, 1969; Longuet-Higgins, 1972). Outside the surf zone S_{yx} is conserved, and is given by the relation

$$S_{yx} = En \cos\alpha \sin\alpha = (En \cos\alpha \sin\alpha)_o = \text{const} \qquad (4\text{-}3)$$

S_{yx} is obtained by integrating the energy, E, in the directional spectra with respect to $\cos\alpha \sin\alpha$ to obtain relation (4-3) for each 17-minute run.

The wave energy at the breakpoint was obtained by refracting each frequency band to an estimated breaker depth using Snell's law and relation (4-2). The actual breaker depth was then computed by combining equation (4-1) relating energy and wave height with the criterion for a breaking solitary wave, $\gamma_b = (H/h)_b = 0.78$ (Munk, 1949), and then recomputing the energy at the breakpoint, where h is the depth of water.

Wave heights at the breakpoint depth were then computed using equation (4-1); the radiation stress, S_{yx}, from equation (4-3). The phase velocities at the breaker depth were computed from the Boussinesq dispersion relation (Whitham, 1974, p. 462):

$$C_b^2 = \frac{gh_b}{1 + \frac{1}{3}(kh)_b^2} \qquad (4\text{-}4)$$

It was then possible to estimate the power expended by the waves, $(CS_{yx})_b$ which has been related to the sand transport rate (Figure 6-1). Measured and computed wave parameters are summarized in Table 4-1.

Table 4-1. Forcing Functions

	11 March 77		6 December 78	
h (m)	Array 9.3 m	Breakpoint h_b = 1.43m	Array 6.0 m	Breakpoint h_b = 1.65m
α (degrees) Range	5.3-7.0	2.9-4.1	3.5-8.0	2.0-5.8
Mean	6.0	3.4	5.4	3.4
C (m/sec)	9.1-9.3	3.7-4.6	7.40-7.54	3.2-4.0
	9.2	3.9	7.5	3.6
Cn (m/sec)	8.5-8.7	3.7-4.6	6.90-7.03	3.2-4.0
	8.6	3.9	7.0	3.6
H (m)	0.67-0.83	0.99-1.19	0.91-0.97	1.26-2.70
	0.78	1.12	0.94	1.29
E ($\frac{joules}{m^2}$)	555-853	1198-1725	1008-1186	2089-2768
	742	1529	1090	2483
Syx ($\frac{joules}{m^2}$)	67.0-95.4	78.7-119.3	81.9-129.6	90.7-159.0
	72.1	90.5	95.3	147.0
CSyx ($\frac{watts}{m}$)	624-868	291-537	617-976	290-636
	663	353	715	529

CURRENTS

The general circulation of water in the surf zone, although complex, appears to follow patterns shown schematically in Figure 4-3. Early measurements showed that outside the surf zone, and between rip currents, water tended to move onshore from surface to bottom (Shepard and Inman, 1950). However, inside the surf zone, surface, mid-depth, and bottom waters have different net directions: the surface water moves onshore and longshore and has the greatest speed; the mid-depth water moves on-offshore with a net longshore motion; while the bottom water has a very slow net offshore motion, even though the highest velocities during the passage of a bore are decidedly onshore. There is also an upward circulation associated with the passage of the breaking wave and its bore (Inman and Quinn, 1952; Inman and Nasu, 1956; Inman et al, 1971).

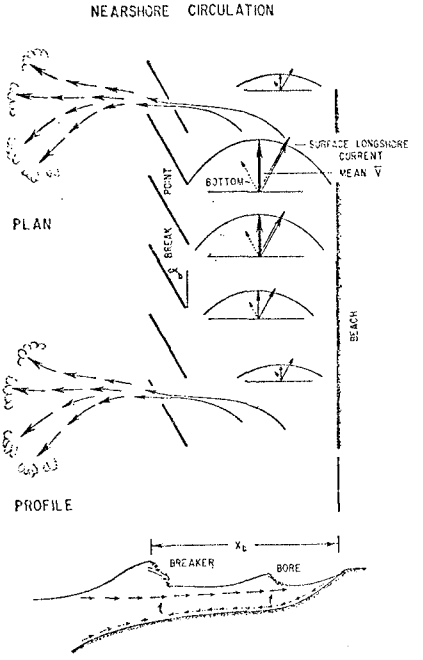

Fig. 4-3 Schematic of surf zone circulation.

Surf zone currents in these studies were measured by three separate methods: 1) dye injection into the water; 2) weighted drift bottles; and, 3) electromagnetic current meters mounted at mid-depths in the surf zone. The first method gives a pattern of water motion and was particularly effective in locating rip currents (Figures 4-4). Drift bottles give Lagrangian trajectories which can be plotted as current velocities representative of the upper layers of the surf zone. The current meters give continuous measures of values of x-y current components, and are most representative of the mid-depth motion of the surf zone (Figures 4-5, 6). They are more fully described by Guza and Thornton (1978).

5. SEDIMENT RESPONSE

The sediment response to the action of waves and currents is complex and not understood. For our purposes we will group these complex motions into bed and suspended load components. Bed load is arbitrarily defined as sand transported on and within 10 cm of the bed; while

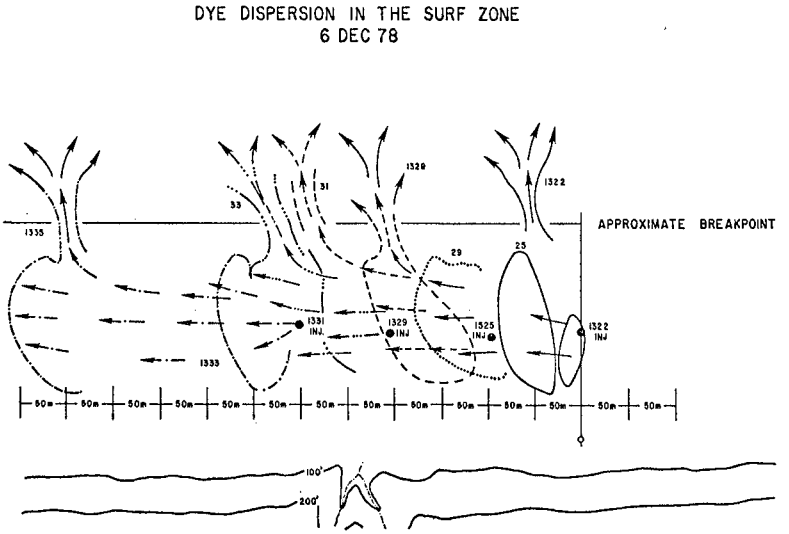

Fig. 4-4 Dye pattern from 13:22 injection.

suspended load is that transported in the water column from 10 cm to the water surface. This definition is used because our present suspended load samplers do not function properly when operated closer to the bed than 10 cm.

TRACER TECHNIQUE FOR BED LOAD

The only known means of estimating the "instantaneous" bed load transport in the field is by tagging the sand in some detectable manner and injecting the tracer into the surf zone (e.g., Inman and Chamberlain, 1959). More recently, flourescent dyed sand grains have been used as tracers by several investigators (Aibulatov, 1961; Ingle, 1966; Komar and Inman, 1970) to study the motion of sand in the nearshore environment. The longshore transport of sand has been estimated by multiplying the rate of advection of sand tracer by the depth in the bed to which the sand tracer mixes (Inman, et al, 1968; Komar and Inman, 1970).

If sand motion consisted of uniform advection, then a line source of tracer sand placed across the surf zone would move at a velocity calculatable directly by sampling the bed at the proper time and distance following injection. However, granular diffusion in the bedload transport, turbulent diffusion in suspended load transport, and non-uniform advection tend to disperse as well as advect the original distribution of tracer. In view of these processes, a concentration-weighted mean velocity must be calculated in order to estimate the true advection rate of tracer and its admixed sand aggregate.

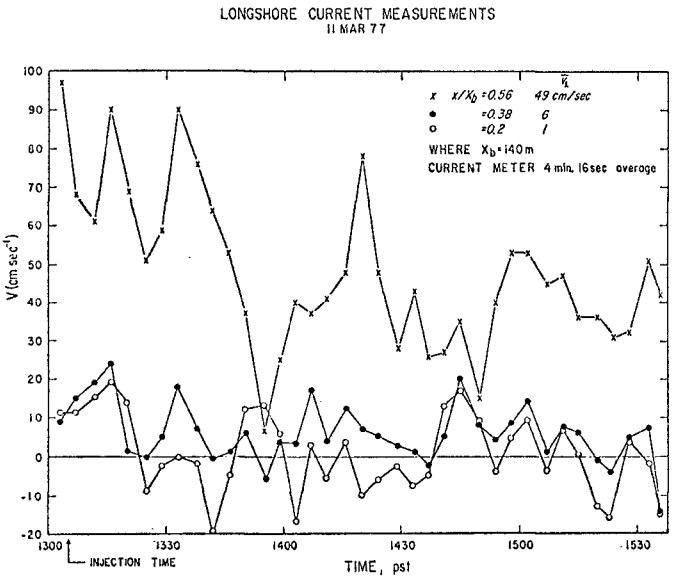

Fig. 4-5 Longshore currents from current meter array for 11 March 1977.

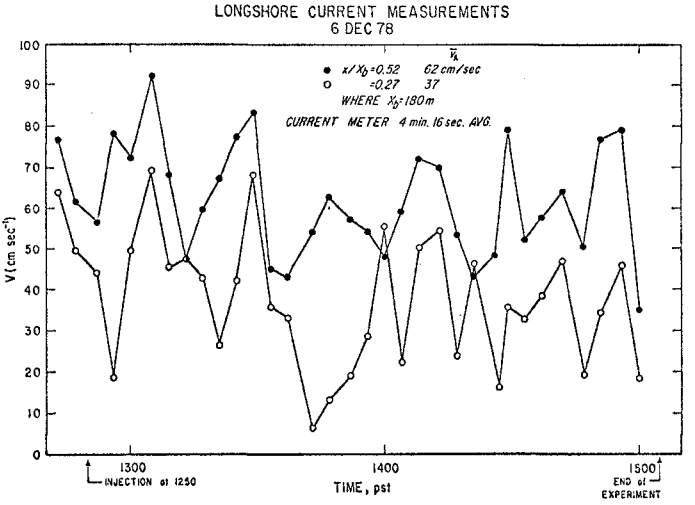

Fig. 4-6 Longshore currents from current meter array for 6 December 1978.

The tracer grain distribution was sampled following injection by two independent methods. The first method uses traditional "grab samplers" designed to sample the upper 2 cm of the sand bed, with the objective of surveying downcurrent as rapidly as possible to give a synoptic areal view of the tracer distribution at a given time. This method is referred to as "spacial sampling." The second method uses specially designed coring devices to repeatedly core the bottom along a fixed on-offshore range, downstream from the injection line and at constant intervals of time, and is analogous to sampling a dye plume in a river as it flows under a bridge. This method is called "temporal sampling." Each sample provides an estimate of the rate of advection. If a sample i is taken y_i meters from the injection line at an elapsed time t_i seconds after injection, then the sand velocity is given by $V_i = y_i/t_i$. If N_i is the tracer concentration of the sample, then a concentration weighted mean advection rate for sand in the longshore direction is given by

$$\bar{V}_\ell = \sum_{i=1}^{n} \left[N \frac{y}{t}\right]_i \Bigg/ \sum_{i=1}^{n} N_i \qquad (5\text{-}1)$$

where n is the total number of samples. This definition of the advection rate V is also time weighted, thus freeing the transport calculation from bias introduced because all of the spacial samples cannot be taken at the same time. Spacial and temporal sampling concepts are shown schematically in Figure 5-1.

Tracer Layer Thickness

The vertical distribution of tracer in the cores was examined to determine the "tracer layer thickness," one of the most uncertain parameters in previous studies (Komar and Inman, 1970). Ideally the measured thickness is one which predicts the actual transport rate when multiplied by the advection rate and surf width. However, the determination of the tracer layer thickness from the core data has been highly subjective. In an effort to remove some of the subjectivity, we have chosen a concentration weighted depth to represent the "tracer layer thickness" Z_o, defined as

$$Z_o = 2 \frac{\int_{z=0}^{\ell} N(z)\, z\, dz}{\int_{z=0}^{\ell} N(z)\, dz} \qquad (5\text{-}2)$$

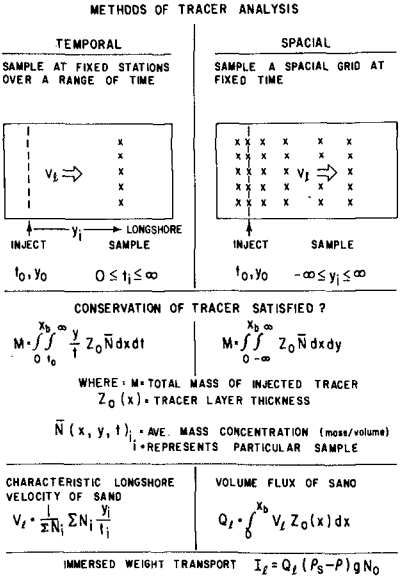

Fig. 5-1

where z is the depth in the bed, N(z) is the tracer concentration at depth z, and ℓ is a depth in the bed greater than any tracer penetrates. It has been assumed here that the surface of the bed (z = 0) is fixed, with no erosion or accretion occurring. We realize that this definition is itself highly subjective, but it is an effort towards standardizing the determination of the tracer layer thickness. It is to be noted that the actual value of Z_o can be greater than the measured value, and the velocity V_ℓ must grade from a maximum at the surface to zero at the bottom of the layer.

The longshore series of cores taken with the center grab sample on 11 March 1977 were analyzed for tracer layer thickness Z_o using several systems including relation (5-2), and the results are plotted in Figure 5-2. The upper curve showing maximum thickness of tracer penetration more closely approximates the thickness used in previous studies (Komar and Inman, 1970); while the lower curve represents a more conservative cut-off thickness where the tracer concentration is 1 grain/gm or less.

BED LOAD TRANSPORT

The product of the tracer layer thickness Z_ℓ, the advection rate of sand and tracer $\bar{V}_\ell$, and the surf zone width X_b, results in an estimate of the longshore bed load sediment transport rate. This procedure is schematically depicted in Figure 5-1.

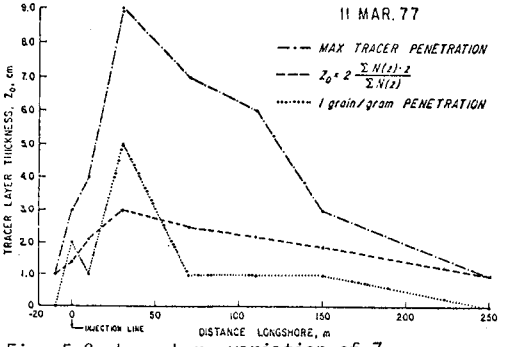

Fig. 5-2 Longshore variation of Z_o

Tracer injections and bed load sampling were made on 11 March 1977 and 6 December 1978. On 11 March 1977, since only spacial sampling was attempted, a grid of 10 X 18 = 180 grab samples were recovered and 21 core samples. The grid is shown in Figure 2-1 and the contours of tracer concentration in Figure 5-3. On December 1978 two spacial and a temporal sampling were made, and the results are shown in Figure 5-4, 5. This procedure permits three independent estimates of transport, but with the same number of personnel, necessarily results in fewer samples per run.

The tracer layer thickness Z_ℓ as a function of surf zone width for both days is plotted in Figure 5-6. It is apparent that Z_ℓ is greatest in the swash zone and least in the central portion of the surf zone, and again increases towards the breakpoint. Separate investigation, not reported here, confirms this bimodal distribution of Z_ℓ, i.e., minimum values in the center of the surf zone. This bimodality was used to estimate transport rates near the breakpoint on these high energy days where breakpoint samples were not obtained.

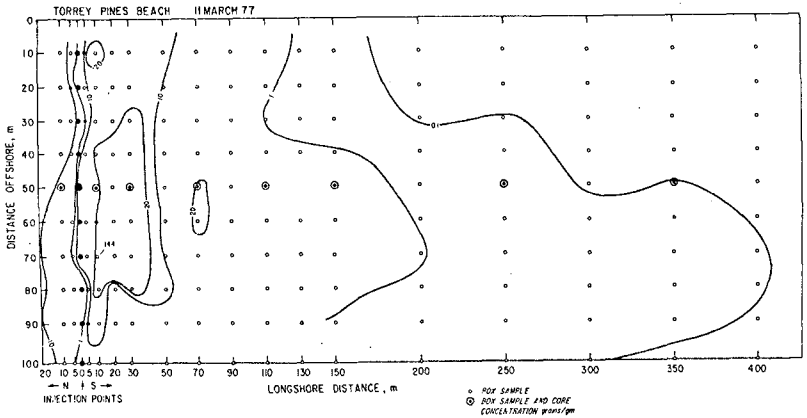

Fig. 5-3 Distribution of grab sample tracer concentrations on 11 March 77.

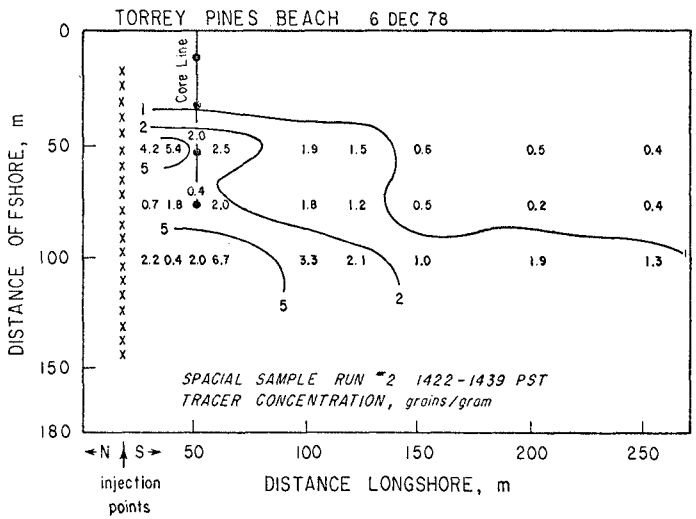

Fig. 5-4 Distribution of grab sample tracer concentrations on 6 December 78.

Three types of estimates for the transport rate were made in order to demonstrate the effect of the conceptual models in the interpretation of field data. The first estimate used the tracer layer thickness, Z_o, as defined in eq. 5-2 and assigned the mid-surf value of Z_o to the unsampled outer portion of the surf zone. The second estimate extrapolated the tracer layer thickness to the unsampled portion of the surf-zone using a bimodal distribution as described above. The final estimate equated Z_o to the maximum thickness of tracer penetration and applied a bimodal distribution for the tracer layer thickness.

The percent recovery of tracer was calculated for both spacial and temporal methods. For the spacial method, each sample yields an estimate for the total amount of tracer in the region from which it was taken. These estimates can be summed over the experimental grid and compared with the known quantity of tracer injected over the same area. For the temporal method, the amount of tracer which advected across the sampling line is estimated, and compared to the amount of tracer injected in that portion of the surf zone covered by the temporal sampling line.

Table 5-1. Sediment Response

	11 March 77	6 December 78		
		Spacial		Temporal
		Run #1	Run #2	
Sampling Start (min. after inj.)	85	41	92	15
Sampling End (min. after inj.)	170	71	109	135
Tracer Recovery (%)	65	39	77	48
Immersed Wt. Longshore Transport Rate, I_ℓ (nt/sec)				
1) Initial Estimate & Eq. 5-2	92	142	167	285
2) Bimodal Z_o & Eq. 5-2	150	179	211	359
3) Max. Tracer Penetration & Bimodal Distribution	474	240	283	481
Suspended Load (nt/sec)				
Under Crest	34	60		
Average	23	33		
Tracer Amount Injected (kg)	113	90.7		
Surf Zone Width (m)				
Range	125-150	150-200		
Significant X_b	140	180		

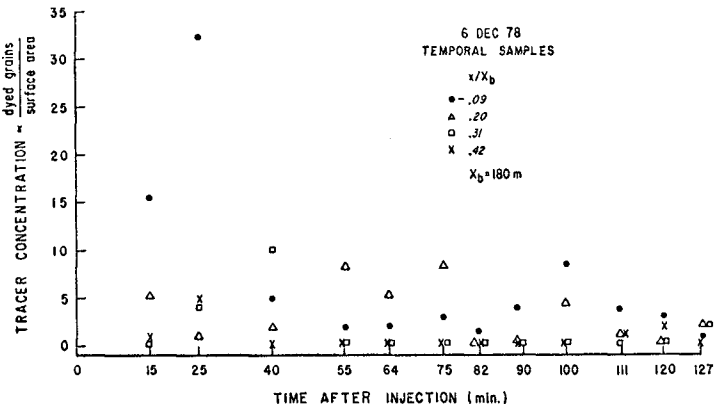

Fig. 5-5 Variation of core line tracer concentration with time after injection.

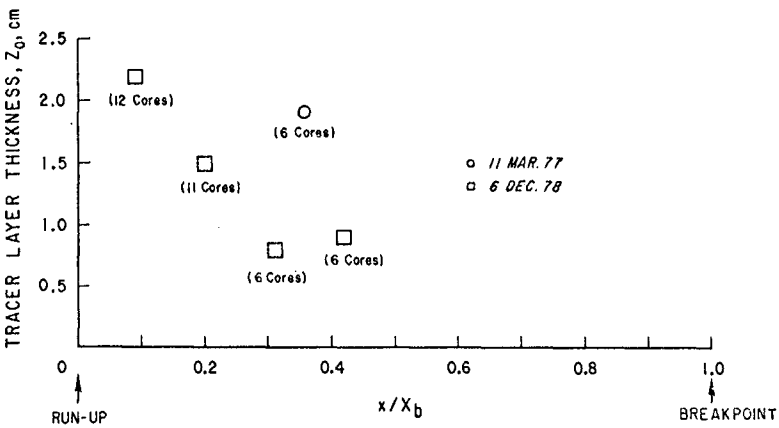

Fig. 5-6 On-offshore variation of tracer layer thickness (Z_o).

SUSPENDED LOAD

Suspended sediment samples were collected on 11 March 1977 and 6 December 1978 during the period between tracer sand injection and the start of grab sampling. The 11 March 1977 samples were collected at the offshore positions shown in Figure 5-7. Six sample series were collected below the crest of the bore, five series between bores, and five just before passage of the bore. On 11 March 1977 samples were taken where bore heights ranged from 30 cm to 102 cm. The breaker type on 11 March 1977 ranged from spilling to plunging, with some strongly plunging.

During the 6 December 1978 experiment suspended sediments were collected at four stations from under the passing crest of the bore. Because of high plunging breakers, these samples did not extend beyond the inner surf zone (Figure 5-8). Samples were collected under bores ranging in height from 49 to 72 cm on that day, with a total range of heights during the November-December 1978 experiments of 15 to 131 cm.

The suspended load was integrated over depth to give the suspended load in grams over a square meter of bed. The product of this load and the average longshore current was then assumed to give an estimate of the suspended load transport rate for that portion of the surf zone. These estimates, when integrated across the surf zone, give the estimates of total suspended load transport rate. The 11 March 1977 experiment provides data on the variation of suspension over a wave cycle. On this day the average suspended load over a wave was used to estimate the total suspended load transport rate. The 6 December 1978 rates were corrected using information from the 11 March 1977 experiement. The total suspended load transport rates are listed in Table 5-1..

FIELD AND LABORATORY PROCEDURES

The tracer experiment used natural Torrey Pines Beach sand dyed with either Florescein (green) of Rhodamine (red) dye. Plastic bags of wetted tracer sand were placed on the sand bed along the injection range to approximate a line source of tracer across the surf zone; then each bag was emptied simultaneously at the time of injection.

The grab samples were collected using a hand-held, scissors type, box grab sampler with the sample volume of 7.5 x 12.5 and 2.1 cm deep. The samples were transferred to plastic bags and labeled with date and grid location. Grab and core samplers were designed for both simplicity of operation in the surf zone and for recovery of sediment cores with undisturbed vertical structure, described in Waldorf and Zampol(in prep).

In the period between injection of tracer and grab sampling, the suspended load was sampled at a number of points across the surf zone. At each sample location a vertical series of 3 or 4 suspended load samples were taken using a "water-coring device" (Waldorf and Zampol, in prep). The swash was sampled with a mechanically closed "plastic bag" sampler.

After fresh water rinsing and drying, 10 gram sub-samples from each grab sample were spread to a single grain layer thickness on a counting grid. The fluorescent tracer grains in the sample were counted using a long-wave ultraviolet light in a completely darkened room. Using these techniques, tracer concentrations as low as 100 grains/kg are measured.

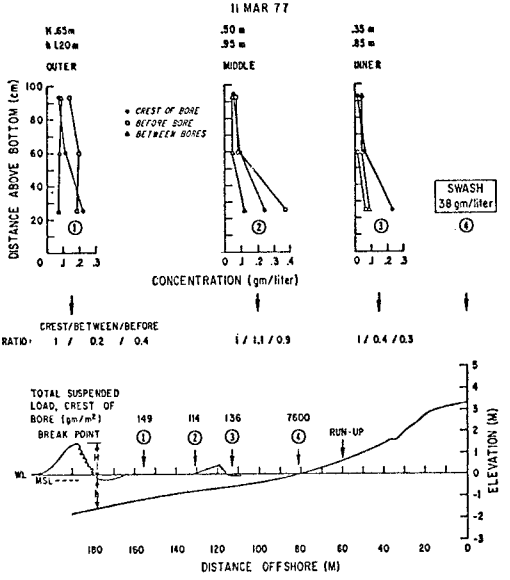

Fig. 5-7 Representative suspended load, profiles, and sampling locations for 11 March 77.

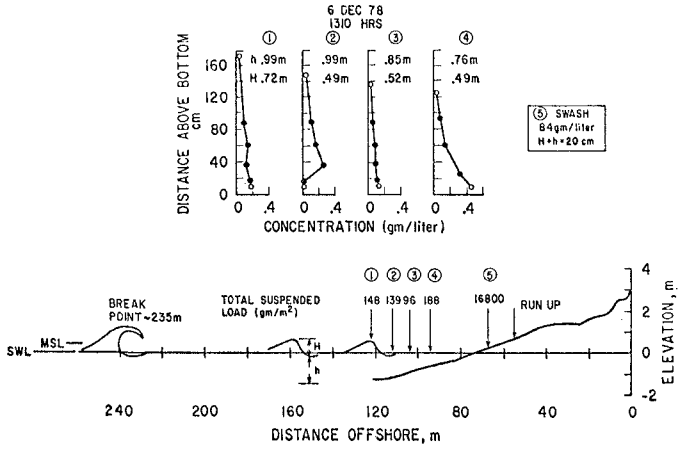

Fig. 5-8 Representative suspended load, profiles, and sampling locations for 6 December 78.

6. DISCUSSION

The bed and suspended load measurements presented here were made under the most intensely monitored forcing conditions yet reported for moderately high energy, dissipative beaches (gentle slope, wide surf zone). As a consequence more surf zone variables and their ranges are known than for previous field investigations. The measurements also showed some trends suggesting that previous simplistic models and methods of calculation should be revised.

FORCING FUNCTIONS

The surf zone width X_b varies with breaker height and type, and a rigorous definition is not generally possible. However, the old concept of a "significant surf zone width" determined by the average of the one-third highest breakers seems appropriate from the standpoint of energy and momentum fluxes.

The complex nature of the longshore and the on-offshore currents was clearly demonstrated by the three methods of current measurement employed, and portrayed schematically in Figure 4-3. The strongest currents were always near the midpoint of the surf zone, and no dyed water passed seaward of the breakpoint except in rip currents. Rip currents may be stationary (Figure 2-1), or may progress down current through the experiment area as in Figure 4-5. The effect of rip currents on the overall transport is not known, but must be considered as an important mechanism in the overall transport processes.

SEDIMENT RESPONSE

The on-offshore bimodality of the tracer layer thickness Z_o was an unexpected finding, and clearly emphasizes the shortcoming of basing transport estimates on limited core information. The concepts of "tracer layer thickness" are of sufficient importance to merit much of the discussion in Section 5, and resulted in the definition given in relation (5-2). The differences between this definition and others is shown graphically by Figure 5-2. The upper curve of maximum tracer penetration more closely approximates the value of tracer layer thickness used previously by Inman et al (1968) and Komar and Inman (1970). Since the interpretation of sand tracer data depends upon the conceptual models of the processes involved, we have interpreted the data in accordance with several models in order to demonstrate the ranges in sand transport rates to be expected. For purposes of comparison, transport estimates are plotted together with the previous data of Komar and Inman (1970) in Figure 6-1.

The difference in transport rates between the spacial and temporal sampling on 6 December 1978 is not clear. However, the persistence of rip currents moving through the sampling grid (Figure 4-5) suggest tracer was lost offshore. This effect would be more pronounced in the spacial sampling which is sensitive to the entire grid length, than to the temporal sampling which was relatively close to the injection point (Figure 5-4). If this is the cause for the different transport rates, then the temporal sampling is the more accurate value.

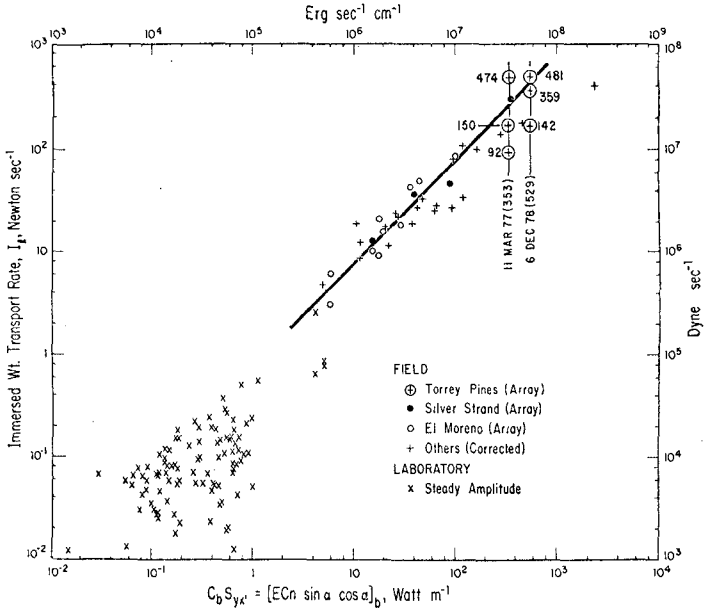

Fig. 6-1 Wave power vs. sediment transport rate (after Komar and Inman, 1970). Ranges of values for 11 March 77 and 6 December 78 are indicated.

Suspended load measurements emphasized the complex nature of suspension processes and demonstrate the need for continuous monitoring sensors vs. the discrete type samplers employed here. Even so, these data show the importance of the changes in concentration as a function of the phase of the bore. Other data taken during the 1977-78 period by this laboratory indicate the importance of the type of breaking wave. Plunging waves suspend much more sediment than spilling waves, especially near the breakpoint. There also appears to be a bimodal distribution of suspension, with maxima in the swash zone and near the breakpoint. The ratio of suspended transport rate to tracer-determined transport rate is 10 to 20% on 11 March 1977 and 6 December 1978. Thus, a comprehensive model of longshore transport as well as on-offshore transport will need to incorporate suspended load as a fundamental component of the total load.

REFERENCES

Aibulatov, N.A., 1961, "Quelques données sur le transfert des sédiments sableux le long d'un littoral, obtenues à l'aide de luminophores," Cahiers Oceanog., 13:292-300.

Bowen, A.J., 1969, "The generation of longshore currents on a plane beach," Jour. of Marine Research, 27, 2:125-206.

Capon, J., 1969, "High resolution frequency-wavenumber spectrum analysis," Proc. IEEE, 57:1408-1418.
Chamberlain, T.K., 1960, "Mechanics of mass sediment transport in Scripps Submarine Canyon," Ph.D. thesis, Univ. of Calif., San Diego, 200 pp.
Davis, R.E. and L.A. Regier, 1977, "Methods for estimating wave spectra," Jour. of Marine Research, 35, 3:454-477.
Gable, C.G., 1979, "Report on data from the Nearshore Sediment Transport Study experiment at Torrey Pines Beach, Calif., November-December 1978," Institute of Marine Resources, IMR Reference No. 79-8.
Guza, R.T. and E.B. Thornton, 1978, "Variability of longshore currents," Proc. 16th Coastal Eng. Conf., Amer. Soc. Civil Eng., 756-775.
_____, 1980, "Local and shoaled comparisons of sea surface elevations, pressures and velocities," Jour. Geophys. Res., 85, C3:1524-30.
Ingle, J.C., Jr., 1966, "The movement of beach sand," Developments in Sedimentology, 5, Elsevier Publ. Co., New York, 221 pp.
Inman, D.L., 1952, "Measures for describing the size distribution of sediments," Jour. Sed. Pet., 22:125-145.
_____ and T.K. Chamberlain, 1959, "Tracing beach sand movement with irradiated quartz," Jour. Geophys. Res., 64, 41-47.
_____, P.D. Komar and A.J. Bowen, 1968, "Longshore transport of sand," Proc. 11th Coastal Eng. Conf., Amer. Soc. of Civil Eng., 1:298-306.
_____ and N. Nasu, 1956, "Orbital velocity associated with wave action near the breaker zone," Beach Erosion Board, Tech Memo 79,72 pp.
_____ and W.H. Quinn, 1952, "Currents in the surf zone," Proc. 2nd Coastal Eng. Conf., Council on Wave Research, Univ. of Cal.,24-36.
_____, R.J. Tait and C.E. Nordstrom, 1971, "Mixing in the surf zone," Jour. Geophys. Res., 76, 15:3493-3514.
Komar, P.D. and D.L. Inman, 1970, "Longshore sand transport on beaches," Jour. Geophys. Res., 75, 30:5914-27.
Longuet-Higgins, M.S., 1972, "Recent progress in the study of longshore currents," Waves on Beaches and Resulting Sediment Transport, Academic Press, New York and London, 203-248.
Lowe, R.L., D.L. Inman and B.M. Brush, 1973, "Simultaneous data system for instrumenting the shelf," Proc. 13th Coastal Eng. Conf., Amer. Soc. of Civil Eng., 95-112.
Munk, W.H., 1949, "The solitary wave theory and its application to surf problems," Ann. N.Y. Acad. Sci., 51:376-424.
Seymour, R.J. and C.G. Gable, 1980, "Nearshore Sediment Transport Study Experiments," Proc. 17th Coastal Eng. Conf., Amer. Soc. of Civil Engrs., in press.
Shepard, F.P. and D.L. Inman, "Nearshore water circulation related to bottom topography and wave refraction," Trans., Amer. Geophys. Union, 31, 2:196-212.
State of Calif., 1969, "Interim Report on Study of Beach Nourishment Along the Southern Calif. Coastline," Dept. of Water Resources, Southern District, Sacramento, Calif.
Whitham, G.B., 1974, Linear and Nonlinear Waves, John Wiley and Sons, New York, 636 pp.